Squark-, slepton-, and neutralino-chargino coannihilation effects in the low-energy effective minimal supersymmetric standard model

V. A. Bednyakov*
Laboratory of Nuclear Problems, Joint Institute for Nuclear Research, 141980 Dubna, Russia

H. V. Klapdor-Kleingrothaus and V. Gronewold
Max-Planck-Institut für Kernphysik, Postfach 103980, D-69029, Heidelberg, Germany
(Received 23 August 2002; published 27 December 2002)

We calculate the neutralino relic density within the low-energy effective minimal supersymmetric extension of the standard model (effMSSM) taking into account slepton-neutralino, squark-neutralino and neutralino–chargino-neutralino coannihilation channels. By including squark (top squark and bottom squark) coannihilation channels we extend our comparative study to all allowed coannihilations and obtain the general result that all of them give sizable contributions to the reduction of the neutralino relic density. Because of these coannihilation processes some models (mostly with large neutralino masses) fall within the cosmologically interesting region for relic density, but other models drop out at this region. Nevertheless, the predictions for direct and indirect dark matter detection rates are not strongly affected by these coannihilation channels in the effMSSM.

DOI: 10.1103/PhysRevD.66.115005 PACS number(s): 11.30.Pb, 12.60.Jv, 95.35.+d

I. INTRODUCTION

A variety of data, ranging from galactic rotation curves to large scale structure formation, and the cosmic microwave background radiation imply a significant density $0.1<\Omega h^2<0.3$ [1] of so-called cold dark matter (CDM). Here $\Omega=\rho/\rho_c$ and $\rho_c=3H^2/8\pi G_N$ is the critical closure density of the universe, G_N is the Newton constant, and h is the Hubble constant in units of 100 km/s/Mpc. It is generally believed that most of the CDM is made of weakly interacting massive particles (WIMPs) [2]. A commonly considered candidate for the WIMP is the lightest neutralino, provided it is the lightest supersymmetric particle (LSP) [3] in the minimal supersymmetric extension of the standard model (MSSM). Four neutralinos in the MSSM, being mass eigenstates, are mixtures of the B-ino $\tilde{B}$, W-ino $\tilde{W}$, and Higgsinos $\tilde{H}_d^0$, $\tilde{H}_u^0$, and the LSP can be written as a composition $\chi\equiv\tilde{\chi}_1=N_{11}\tilde{B}+N_{12}\tilde{W}+N_{13}\tilde{H}_d^0+N_{14}\tilde{H}_u^0$, where N_{ij} are the entries of the neutralino mixing matrix. In supersymmetry (SUSY) phenomenology one usually classifies neutralinos as gaugino-like (with $\mathcal{P}\approx 1$), Higgsino-like (with $\mathcal{P}\approx 0$), and mixed, where the gaugino fraction is defined as $\mathcal{P}=|N_{11}|^2+|N_{12}|^2$.

In most approaches the LSP is stable due to R-parity conservation [4]. The neutralino, being massive, neutral and stable, often provides a sizable contribution to the relic density. The contribution of neutralinos to the relic density is strongly model dependent and varies by several orders of magnitude over the whole allowed parameter space of the MSSM. The neutralino relic density then can impose stringent constraints on the parameters of the MSSM and the SUSY particle spectrum, and may have important consequences both for studies of SUSY at colliders and in astroparticle experiments. In light of this and taking into account the continuing improvements in determining the abundance of CDM and other components of the Universe, which have now reached an unprecedented precision [5], one needs to perform an accurate enough computation of the WIMP relic abundance, which would allow reliable comparison of theory with observation. Important progress in calculations of the relic density of neutralinos in a variety of supersymmetric models has been already made [6–42].

In the early universe neutralinos existed in thermal equilibrium with the cosmic thermal plasma. As the universe expanded and cooled, the thermal energy is no longer sufficient to produce neutralinos at an appreciable rate, they decouple and their number density scales with co-moving volume. The sparticles significantly heavier than the LSP decouple at an earlier time and decay into LSPs before the LSPs themselves decouple. Nevertheless there may exist some other next-to-lightest sparticles (NLSPs) which are not much heavier than the stable LSP. The number densities of the NLSPs have only slight Boltzmann suppressions with respect to the LSP number density when the LSP freezes out of chemical equilibrium with the thermal bath. Therefore they may still be present in the thermal plasma, and NLSP-LSP and NLSP-NLSP interactions keep the LSP in thermal equilibrium, resulting in significant reduction of the LSP number density and leading to acceptable values even with a rather heavy sparticle spectrum [26]. These *coannihilation* processes can be particularly important when the LSP-LSP annihilation rate itself is suppressed [14,39,23]. Any SUSY particle can be involved in the coannihilation process provided its mass is almost degenerate with the mass of the LSP [14,27]. In the low-energy effective MSSM (effMSSM), where one ignores restriction from unification assumptions and investigates the MSSM parameter space at the weak scale [23,21,43,44] there is, in principle, no preference for the next-to-lightest SUSY particle.

*Email address: bedny@nusun.jinr.ru

The relativistic thermal averaging formalism [15] was extended to include coannihilation processes in [23], and was implemented in the DARKSUSY code [24] for coannihilation of charginos and heavier neutralinos. In was found [23] that for Higgsino-like LSP such a coannihilation significantly decreases the relic density and rules out these LSPs from the region of cosmological interest.

The importance of the neutralino coannihilation with sfermions was emphasized and investigated for sleptons [26,28], top squarks [33,34] and bottom squarks [31] in the so-called constrained MSSM (CMSSM) [22,16,45] or in supergravity (MSUGRA) models [46]. The most popular MSUGRA model [46] has a minimal set of parameters: m_0, $m_{1/2}$, A_0, $\tan\beta$, and $\mathrm{sgn}(\mu)$. Here m_0 is the universal scalar mass, $m_{1/2}$ is the universal gaugino mass, and A_0 is the universal trilinear mass, all evaluated at M_{GUT}, $\tan\beta$ is the ratio of Higgs field vacuum expectation values, and μ is a Higgs parameter of the superpotential. There are strong correlations of sfermion, Higgs boson, and gaugino masses in MSUGRA originating from unification assumptions. In regions of the MSUGRA parameter space where χ and $\tilde{\tau}_1$ were nearly degenerate (at low m_0), coannihilations could give rise to reasonable values of the relic density even at very large values of $m_{1/2}$, at both low and high $\tan\beta$ [26,31]. In addition, for large values of the parameter A_0 or for non-universal scalar masses, top or bottom squark masses could become nearly degenerate with the χ, so that squark coannihilation processes can become important as well [33,34]. Therefore due to slepton and squark coannihilation effects, the relic density can reach the cosmologically interesting range of $0.1<\Omega h^2<0.3$.

The influence of coannihilation channels on the LSP proton scalar elastic cross sections was considered in supergravity and D-brane models in [31] and in a MSUGRA-like SUSY model for large $\tan\beta$ (only for stau coannihilations) in [29].

Having in mind investigation of future prospects for direct and indirect detection of relict LSP we follow the most phenomenological view, not bounded by theoretical restrictions from sfermion–gaugino–Higgs-boson mass unifications, etc. To this end we need maximally general and accurate calculations of the relic density within the low-energy effective MSSM scheme (effMSSM) [21,43]. The high-level tool for these calculations is the DARKSUSY code [24]. Unfortunately the code calculates only the neutralino with next neutralino(s) and chargino coannihilations (NCC), which is not sufficient, when neutralino-slepton coannihilation (SLC) and neutralino-squark (SQC) coannihilation are claimed to be dominant [26,28,33,34,31].

Contrary to the majority of previous papers (see for example [26,34,30,28,40]), aimed mostly at discovery and demonstration of the importance or dominance of some specific coannihilation channels, our main goal is the investigation of the interplay between different coannihilation channels as well as their consequences for detection of CDM. To this end a comparative study of NCC and SLC channels, exploration of relevant changes in the relic density and investigation of their consequences for detection of CDM particles were performed in the effMSSM in our previous paper [42]. The present paper extends our investigations [42] to the neutralino–top-squark and neutralino–bottom-squark coannihilations and completes our consideration of the subject. For this purpose we combined our previous code [43] with the DARKSUSY code [24] and codes of [26,34], which allows for the first time comparative study of relevant coannihilation channels (NCC, SLC, SQC) in the low-energy effMSSM.

II. THE effMSSM APPROACH

As free parameters in the effMSSM, we use the gaugino mass parameters M_1, M_2, the entries to the squark and slepton mixing matrices $m^2_{\tilde{Q}}, m^2_{\tilde{U}}, m^2_{\tilde{D}}, m^2_{\tilde{R}}, m^2_{\tilde{L}}$ for the first and second generations and $m^2_{\tilde{Q}_3}, m^2_{\tilde{T}}, m^2_{\tilde{B}}, m^2_{\tilde{R}_3}, m^2_{\tilde{L}_3}$ for the third generation, respectively, the third generation trilinear soft couplings A_t, A_b, A_τ, the mass m_A of the pseudoscalar Higgs boson, the Higgs superpotential parameter μ, and $\tan\beta$. To reasonably reduce the parameter space we assumed $m^2_{\tilde{U}} = m^2_{\tilde{D}} = m^2_{\tilde{Q}}$, $m^2_{\tilde{T}} = m^2_{\tilde{B}} = m^2_{\tilde{Q}_3}$, $m^2_{\tilde{R}} = m^2_{\tilde{L}}$; $m^2_{\tilde{R}_3} = m^2_{\tilde{L}_3}$ and have fixed $A_b = A_\tau = 0$ [43]. The third gaugino mass parameter M_3 defines the mass of the gluino in the model and is determined by means of the grand unified theory GUT assumption $M_2 = 0.3 M_3$. The remaining parameters defined our effMSSM parameter space and were scanned randomly within the following intervals:

$$-1\ \mathrm{TeV} < M_1 < 1\ \mathrm{TeV}, \quad -2\ \mathrm{TeV} < M_2, \mu, A_t < 2\ \mathrm{TeV},$$

$$1.5 < \tan\beta < 50, \quad 50\ \mathrm{GeV} < M_A < 1000\ \mathrm{GeV},$$

$$10\ \mathrm{GeV}^2 < m^2_{\tilde{Q}}, m^2_{\tilde{L}}, m^2_{\tilde{Q}_3}, m^2_{\tilde{L}_3} < 10^6\ \mathrm{GeV}^2.$$

We have included the current experimental upper limits on sparticle masses as given by the Particle Data Group [47]. The limits on the rare $b \to s\gamma$ decay [48] following [49] have also been imposed. The calculations of the neutralino-nucleon cross sections and direct and indirect detection rates follow the description given in [3,43].

The number density is governed by the Boltzmann equation [15,23]

$$\frac{dn}{dt} + 3Hn = -\langle \sigma v \rangle (n^2 - n_{\mathrm{eq}}^2) \tag{1}$$

with n either being the LSP number density if there are no other coannihilating sparticles, or the sum over the number densities of all coannihilation partners. The index "eq" denotes the corresponding equilibrium value. To solve the Boltzmann equation (1) one needs to evaluate the thermally averaged neutralino annihilation cross section $\langle \sigma v \rangle$. Without coannihilation processes $\langle \sigma v \rangle$ is given as the thermal average of the LSP annihilation cross section $\sigma_{\chi\chi}$ multiplied by the relative velocity v of the annihilating LSPs

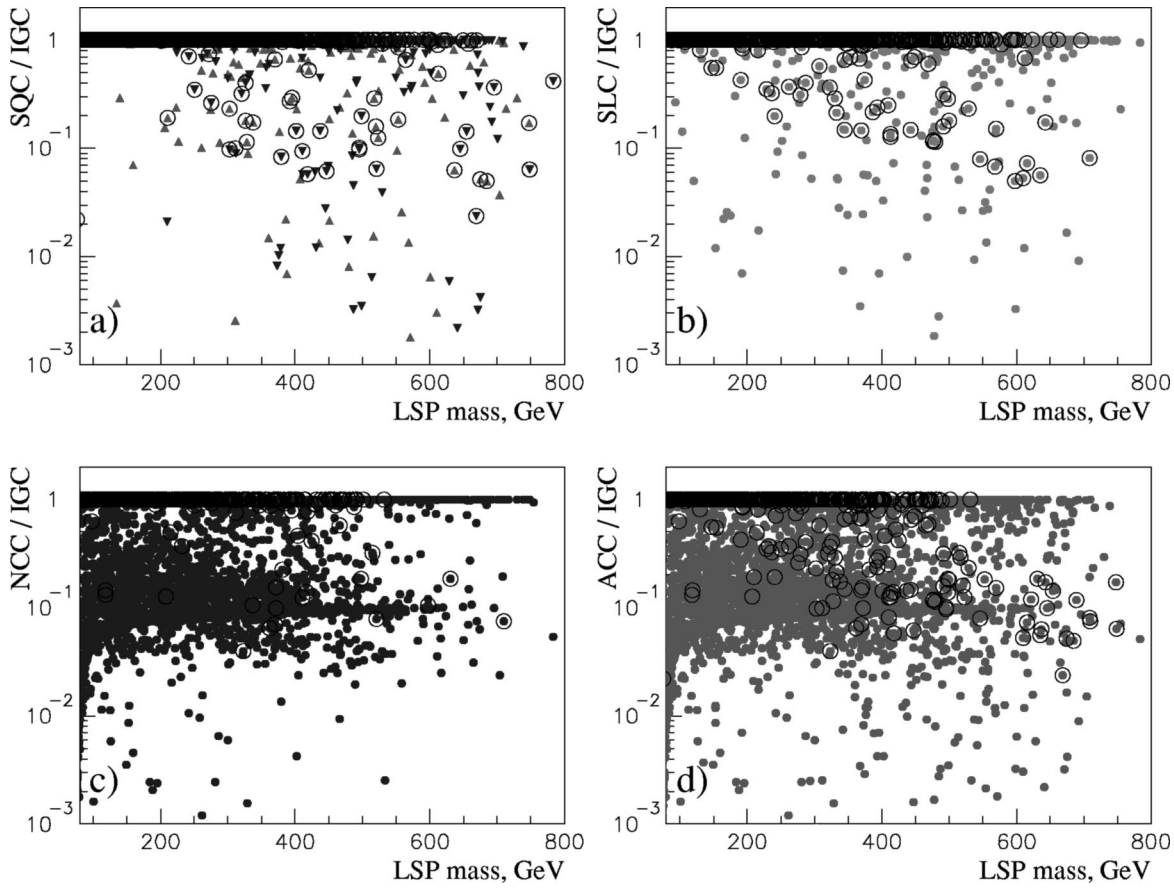

FIG. 1. Effects of squark-neutralino (SQC), slepton-neutralino (SLC), and neutralino-chargino-(neutralino) (NCC) coannihilations in effMSSM. Panels (a)–(d) display ratios $\Omega h^2_{\rm SQC}/\Omega h^2_{\rm IGC}$, $\Omega h^2_{\rm SLC}/\Omega h^2_{\rm IGC}$, $\Omega h^2_{\rm NCC}/\Omega h^2_{\rm IGC}$, and $\Omega h^2_{\rm ACC}/\Omega h^2_{\rm SLC}$ for the case when all coannihilations are included. The maximal reduction factors for all channels (NCC, SQC, and SLC) are of the order of 10^{-3}. Encircled points mark the cosmologically interesting relic density $0.1<\Omega h^2_{\rm COA}<0.3$. In panel (a) up-going triangles correspond to top squark coannihilations and down-going triangles correspond to bottom squark coannihilations. The top squark and bottom squark contributions are seen to be equal.

$$\langle \sigma v\rangle = \langle \sigma_{\chi\chi} v\rangle, \tag{2}$$

otherwise it is determined as $\langle \sigma v\rangle = \langle \sigma_{\rm eff} v\rangle$, where the effective thermally averaged cross section is obtained by summation over coannihilating particles [15,23]

$$\langle \sigma_{\rm eff} v\rangle = \sum_{ij} \langle \sigma_{ij} v_{ij}\rangle \frac{n_i^{\rm eq}}{n^{\rm eq}} \frac{n_j^{\rm eq}}{n^{\rm eq}}. \tag{3}$$

If n_0 denotes the present-day number density of the relics, the relic density is given by

$$\Omega = \frac{m_\chi n_0}{\rho_c}. \tag{4}$$

For each point in the MSSM parameter space (the MSSM model) we have evaluated the relic density of the LSP, ignoring any possibility of coannihilation (IGC), taking into account only neutralino-chargino (NCC), slepton (SLC), or squark (SQC) coannihilations separately, and including all of the coannihilation channels (ACC). To this end DARKSUSY procedures of $\langle \sigma_{\rm eff} v\rangle$ evaluation and solution of Boltzmann equation were implemented in our former code [43]. Coannihilations with two-body final states that can occur between neutralinos, charginos, sleptons, top squarks, and bottom squarks, as long as their masses are $m_i<2m_\chi$, were included. The Feynman amplitudes for NCC, SLC, and top squark coannihilations were taken from DARKSUSY [24], [50,26], and [51,34], respectively. The amplitudes for the bottom coannihilation were obtained on the basis of the top squark amplitudes from [51,34]. As in [42], the $\langle \sigma_{\rm eff} v\rangle$ and Ωh^2 were calculated following the relevant DARKSUSY routines [24] to which the codes [50,26] and [51,34] were added in a way that guarantees the correct inclusion of SLC and SQC.

In the case where all squarks, sleptons, neutralinos, and charginos are substantially heavier than the LSP ($m_i > 2m_\chi$) and there are no possible coannihilations, the relic density $\Omega h^2 = \Omega h^2_{\rm ACC} = \Omega h^2_{\rm NCC} = \Omega h^2_{\rm SLC} = \Omega h^2_{\rm SQC}$ is equal to $\Omega_\chi h^2$ obtained without any coannihilations. When, for example, at least one of the coannihilation channels (NCC, SQC, or SLC) is indeed relevant, the $\Omega h^2_{\rm IGC}$ (ignoring coannihilation) is calculated with

$$\langle \sigma_{\rm eff} v\rangle_{\rm IGC} = \langle \sigma_{\chi\chi} v\rangle \left(\frac{n_\chi^{\rm eq}}{n^{\rm eq}}\right)^2, \tag{5}$$

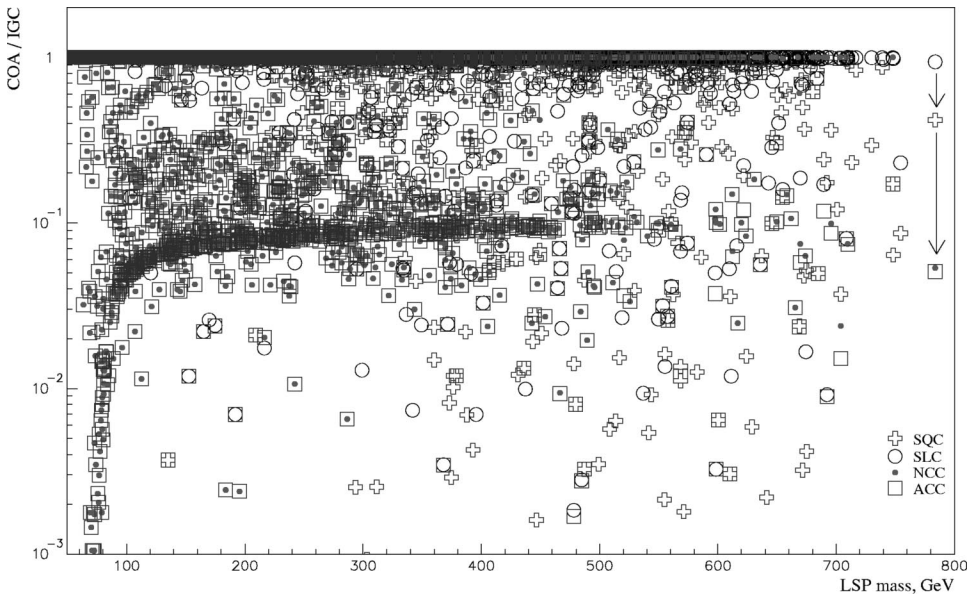

FIG. 2. The same as in Fig. 1, but plotted together. Here $\Omega h^2_{\rm SQC}/\Omega h^2_{\rm IGC}$, $\Omega h^2_{\rm SLC}/\Omega h^2_{\rm IGC}$, $\Omega h^2_{\rm NCC}/\Omega h^2_{\rm IGC}$, and $\Omega h^2_{\rm ACC}/\Omega h^2_{\rm SLC}$ are marked with crosses, circles, dots, and squares, respectively. Therefore, a square filled with a cross, circle, or dot depicts a model that is affected only by SQC, SLC, or NCC, respectively, while any other coannihilation channel gives a negligible contribution. Such a situation takes place for the majority of models, but there are some (very few) models, given by empty squares, for which at least two coannihilation channels are relevant. For example, arrows on the right side of the figure demonstrate how the reduction of the RD proceeds: SLC gives no effect ($\Omega h^2_{\rm SLC}/\Omega h^2_{\rm IGC}=1$), SQC reduces the RD with a factor $\Omega h^2_{\rm SQC}/\Omega h^2_{\rm IGC}\approx 0.4$, and finally NCC gives the main contribution to the RD suppression, $\Omega h^2_{\rm ACC}/\Omega h^2_{\rm SLC}\approx\Omega h^2_{\rm NCC}/\Omega h^2_{\rm IGC}\approx 0.04$ (the square nearly coincides with the dot).

where $n^{\rm eq}$ includes *all* open coannihilation channels. This formula (generalized also for NCC, SLC and SQC) allows a comparative study of all coannihilation channels, always leading to a smaller value for the relic density, $\Omega h^2_{\rm COA}/\Omega h^2_{\rm IGC}<1$. Here $\Omega h^2_{\rm COA}$ is a common notation for $\Omega h^2_{\rm ACC}$, $\Omega h^2_{\rm NCC}$, $\Omega h^2_{\rm SQC}$, or $\Omega h^2_{\rm SLC}$. We assume $0.1<\Omega h^2<0.3$ for the cosmologically interesting region [1].

III. RESULTS AND DISCUSSIONS

A. Coannihilation effects in the relic density

We performed our calculations in the effMSSM approach given above and the results for the neutralino relic density (scatter plots) are presented in Figs. 1–6. The reduction effect on the relic density (RD) produced by SQC, SLC, NCC, and ACC is shown in Fig. 1 as a ratio $\Omega h^2_{\rm COA}/\Omega h^2_{\rm IGC}$. On the basis of our sampling (50000 models tested) the maximum RD suppression factor for the NCC and SLC channels is of the order of 10^{-3}. Almost the same maximal suppression is found for the squark coannihilation channels. These results depend on the experimental limits imposed on the second-lightest neutralino, chargino and slepton top squark and bottom squark masses. If there were no limits on their masses, the factor of relative RD reduction due to NCC could reach a maximum value of 10^{-5} for models with $m_\chi \approx 40$ GeV [42]. The current experimental limits for $m_{\tilde\tau}$, $m_{\tilde\chi^\pm}$, $m_{\tilde t}$, and $m_{\tilde b}$ are 80–90 GeV [47], and therefore the critical LSP mass that enables non-negligible NCC, SLC, and SQC contributions is also of the same order ($m_\chi \geqslant 80$ GeV).

From panel (a) of Fig. 1 one can conclude that top squark (up-going triangles) and bottom squark (down-going triangles) equally contribute to the reduction of the RD due to coannihilations.

The encircled symbols depict some kind of ''constructive'' reduction, when due to the coannihilations the relic density falls into the cosmologically interesting region $0.1<\Omega h^2_{\rm COA}<0.3$. Other points present the cases when coannihilations too strongly reduce the relic density. One can see that NCC plays the main role in the ''destructive'' reduction of RD; these channels reduce the maximal number of models from the cosmologically interesting region [23,42]. Despite this, all coannihilation channels contribute equally in the ''constructive'' reduction of RD [there are almost the same number of the circled points in panels (a)–(c)]. Therefore, for our random sampling in the effMSSM the NCC, SLC, and SQC are indeed relevant ($\Omega h^2_{\rm COA}/\Omega h^2_{\rm IGC}<0.95$) for 2–4 % of models if one assumes $0.1<\Omega h^2_{\rm ACC}<0.3$, and the NCC is indeed relevant for about 30% of models if this constraint is relaxed (Fig. 1).

From Fig. 2 one can see that mainly only one of the coannihilation channels (NCC, SQC, or SLC) dominates in the reduction of the RD. The other channels of coannihilation in general play no role or lead only to a much smaller further reduction [42].

Although other coannihilation processes besides NLSP-LSP can in principal be also open [including the LSP coannihilation with the next-to-NLSP (NNLSP) and next-to-NNLSP, as well as NLSP-NLSP coannihilations, etc.], Fig. 3 allows the conclusion that the dominant coannihilation channel is defined by the type of the NLSP. If the next neutralino

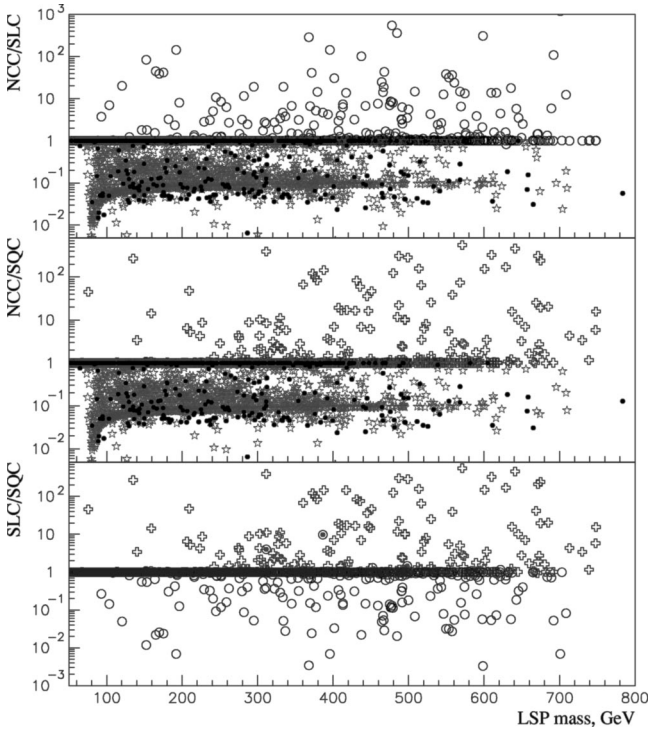

FIG. 3. Ratios $\Omega h^2{}_{\rm NCC}/\Omega h^2{}_{\rm SLC}$, $\Omega h^2{}_{\rm NCC}/\Omega h^2{}_{\rm SQC}$, and $\Omega h^2{}_{\rm SLC}/\Omega h^2{}_{\rm SQC}$ versus m_χ. An open circle indicates that the $\tilde{\tau}$ is the NLSP, the star means that the light chargino $\tilde{\chi}^{\pm}$ is the NLSP, the small filled circle marks the model where the second-lightest neutralino $\tilde{\chi}_2$ is the NLSP. An open cross indicates that the top squark $\tilde{t}$ or the bottom squark $\tilde{b}$ is the NLSP. One sees, for example, that if $\tilde{\chi}_2$ or $\tilde{\chi}^{\pm}$ is the NLSP, the NCC necessarily dominates ($\Omega h^2{}_{\rm NCC}/\Omega h^2{}_{\rm SLC}<1$ or $\Omega h^2{}_{\rm NCC}/\Omega h^2{}_{\rm SQC}<1$) while $\tilde{t}$ or $\tilde{b}$ being the NLSPs always leads to dominant SQC ($\Omega h^2{}_{\rm NCC}/\Omega h^2{}_{\rm SQC}>1$ or $\Omega h^2{}_{\rm SLC}/\Omega h^2{}_{\rm SQC}>1$). The same is in general true for SLC. Circles with dots inside depict models where the NLSP is the stau, but SLC does not dominate.

$\tilde{\chi}_2$ or chargino $\tilde{\chi}^{\pm}$ is the NLSP, then NCC indeed dominates. The SQC dominates when NLSP is the top squark or the sbottom. The stau $\tilde{\tau}$ (or another slepton) being the NLSP entails a dominant SLC effect.

Nevertheless, contrary to the NCC+SLC case [42], there are (very few) models where the stau is the NLSP, but masses of the stau, the top squark and the bottom squark appear by accident almost the same and all of these sparticles participate in the coannihilation with the LSP and each other. As a result, strongly interacting coannihilation channels with squarks produce a larger reduction as compared to the SLC despite the fact that the stau is indeed the NLSP. The bottom panels of Figs. 3 and 4 display an example of such models (circle with a dot inside), in which the stau is the NLSP but the SLC contribution is smaller than the contribution of SQC ($\Omega h^2{}_{\rm SLC}/\Omega h^2{}_{\rm SQC}>1$).

Figure 4 shows that for all coannihilation channels maximal RD reduction factors (less than 0.01) occur for mass differences $m_{\rm NLSP}-m_{\rm LSP}\leqslant 20$ GeV. Mass difference $m_{\rm NLSP}-m_{\rm LSP}\leqslant 5$ GeV plays a significant role in the RD reduction for SLC and mostly for NCC. In contrast with NCC and

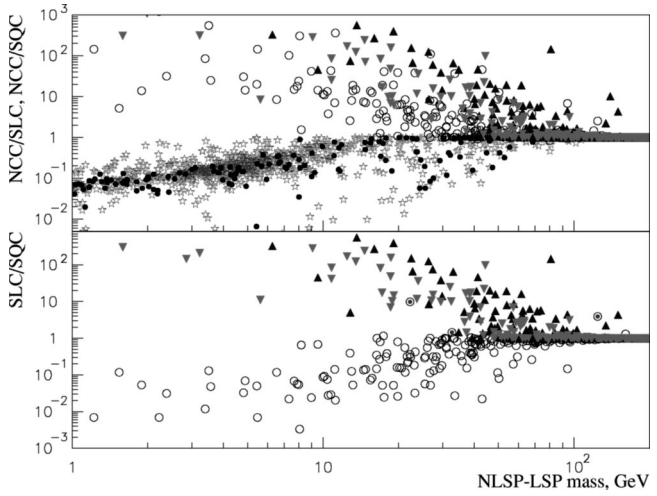

FIG. 4. The same as in Fig. 3, but versus $m_{\rm NLSP}-m_\chi$. Up-going triangles correspond to top squarks and down-going triangles correspond to bottom squarks.

SLC, SQC can produce the same RD reduction effect with larger mass difference between squarks and the LSP ($m_{\tilde{q}}-m_{\rm LSP}\approx 150$ GeV) due to the possibility of coannihilation via the strong interaction.

In the case of SQC the small mass difference between the coannihilating top squark and bottom quarks ($m_{\tilde{t}}-m_{\tilde{b}}$ instead of $m_{\tilde{q}}-m_{\rm LSP}$) can produce a dominant effect in the RD reduction (triangles at $m_{\tilde{q}}-m_{\rm LSP}\geqslant 100$ GeV in Fig. 4 illustrate this possibility).

Although we have set the coannihilation opening threshold of $m_i=2m_\chi$ for NCC and SLC channels, relevant effects occur if the mass difference between the coannihilation partner and the LSP is within 15%. This is in agreement with previous considerations [14,26,30,23,32,28,34,31]. It was found that for SQC the relevant effects occur if the mass difference between the coannihilating squark and the LSP is within 50% (in general agreement with [34,41]).

In Fig. 5 all calculated relic densities ($\Omega h^2{}_{\rm IGC}$, $\Omega h^2{}_{\rm SQC}$, $\Omega h^2{}_{\rm SLC}$, $\Omega h^2{}_{\rm NCC}$, and $\Omega h^2{}_{\rm ACC}$) are depicted in the cosmologically interesting region $0.1<\Omega h^2{}_{\rm COA}<0.3$. A large number of models (mostly with $m_\chi\leqslant 250$GeV) are completely unaffected by any kind of coannihilation. When at least one of the coannihilation channels is relevant, the RD decreases and some cosmologically unviable models with $\Omega h^2{}_{\rm IGC}>0.3$ enter the cosmologically interesting range $0.1<\Omega h^2{}_{\rm COA}<0.3$, due to NCC (squares with a dot inside), SLC (squares with circles inside), SQC (squares with crosses inside), or due to the joint contribution of NCC, SQC, and/or SLC (empty squares).

There are also models which fall within the less interesting region ($\Omega h^2{}_{\rm COA}<0.1$). The largest amount of models are shifted out due to NCC (star-crossed circles), and a relatively small amount of models is shifted out due to SLC (crossed stars with a dot inside), SQC (circles with a star and a dot inside), both NCC and SLC (crossed stars). There are cosmologically interesting LSPs within the full mass range 20 GeV$<m_\chi<$720 GeV (Fig. 5) accessible in our scan whether or not coannihilation channels are included.

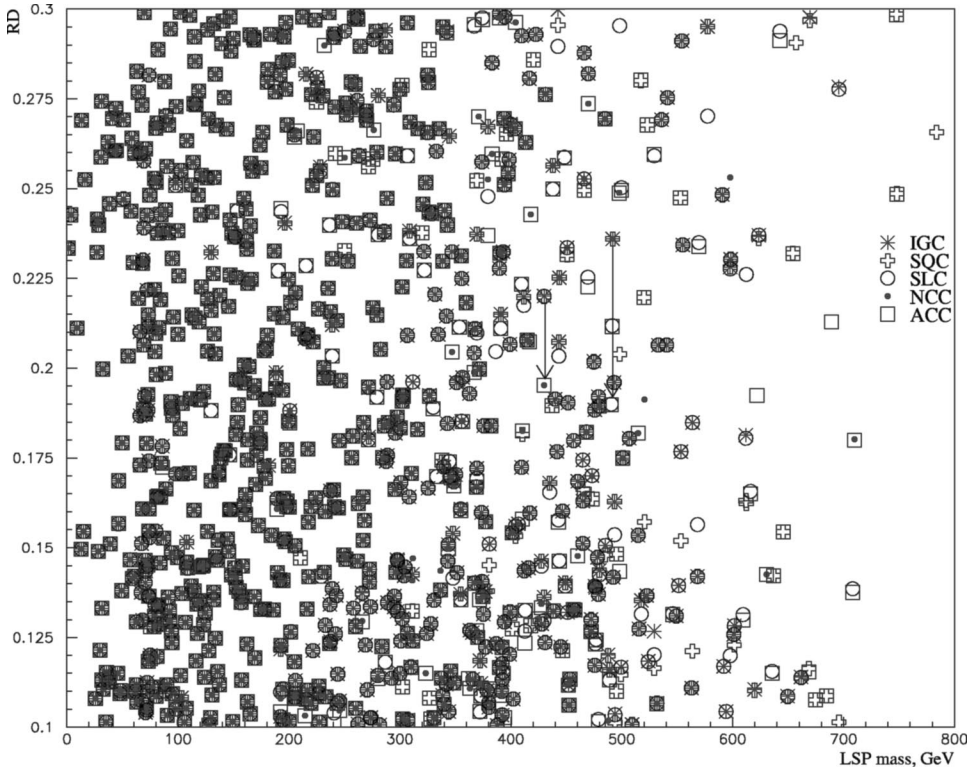

FIG. 5. Illustration of the shifting of effMSSM models into and out of the cosmologically interesting range $0.1<\Omega h^2_{\mathrm{COA}}<0.3$ due to NCC, SQC, and SLC. Relic densities $\Omega h^2_{\mathrm{IGC}}$, $\Omega h^2_{\mathrm{SQC}}$, $\Omega h^2_{\mathrm{SLC}}$, $\Omega h^2_{\mathrm{NCC}}$, and $\Omega h^2_{\mathrm{ACC}}$ are marked with stars, crosses, circles, small dots, and squares, respectively. Therefore, a superposition of all those symbols corresponds to a model which is totally untouched by coannihilation. A star-crossed circle marks a model which is unaffected by SLC and SQC ($\Omega h^2_{\mathrm{SLC}}=\Omega h^2_{\mathrm{SQC}}=\Omega h^2_{\mathrm{IGC}}$), but is shifted down due to NCC. If the corresponding $\Omega h^2_{\mathrm{ACC}}$ (which is equal to $\Omega h^2_{\mathrm{NCC}}$) remains within this range, it is still present in the figure below this star-crossed circle as a square with a black dot inside (see short arrow). By analogy, a square with a circle inside gives a model which is shifted into the region due to SLC only ($\Omega h^2_{\mathrm{ACC}}=\Omega h^2_{\mathrm{SLC}}$), and if the corresponding $\Omega h^2_{\mathrm{IGC}}=\Omega h^2_{\mathrm{NCC}}=\Omega h^2_{\mathrm{SQC}}$ is also in the cosmologically viable range, it is located above the symbol as a crossed star with a dot inside (see long arrow). Quite a large number of models are shifted out of the range $0.1<\Omega h^2<0.3$ due to NCC (star-crossed circles).

Cosmologically interesting LSPs occur with arbitrary compositions when coannihilations are ignored (Fig. 6), the inclusion of NCC rules out all the models with Higgsino-like LSPs (star-crossed circles), SLC and SQC further tends to rule out LSPs with mixed composition, so that only LSPs with $\mathcal{P}>0.67$ [there are no squares for $\mathcal{P}/(1-\mathcal{P})<2$] remain as dominant CDM candidates. In general our estimations (Fig. 6) are in accordance with previous considerations [26,23], as far as they can be compared with these less general treatments.

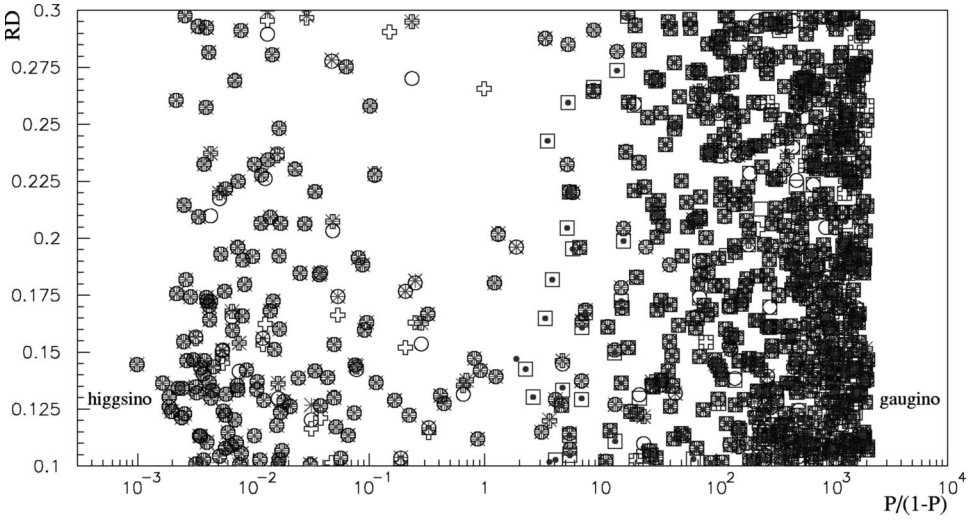

FIG. 6. Variation of relic density against gaugino fraction. As in Fig. 5, the RD $\Omega h^2_{\mathrm{IGC}}$, $\Omega h^2_{\mathrm{SQC}}$, $\Omega h^2_{\mathrm{SLC}}$, $\Omega h^2_{\mathrm{NCC}}$, and $\Omega h^2_{\mathrm{ACC}}$ are marked with stars, crosses, circles, small dots, and squares, respectively. The NCC reduces the RD especially for models with Higgsino-like LSPs and shifts these models out of cosmological interest. The joint effect of NCC, SQC, and SLC leaves only LSPs with $\mathcal{P}>0.67$ in the cosmologically interesting region.

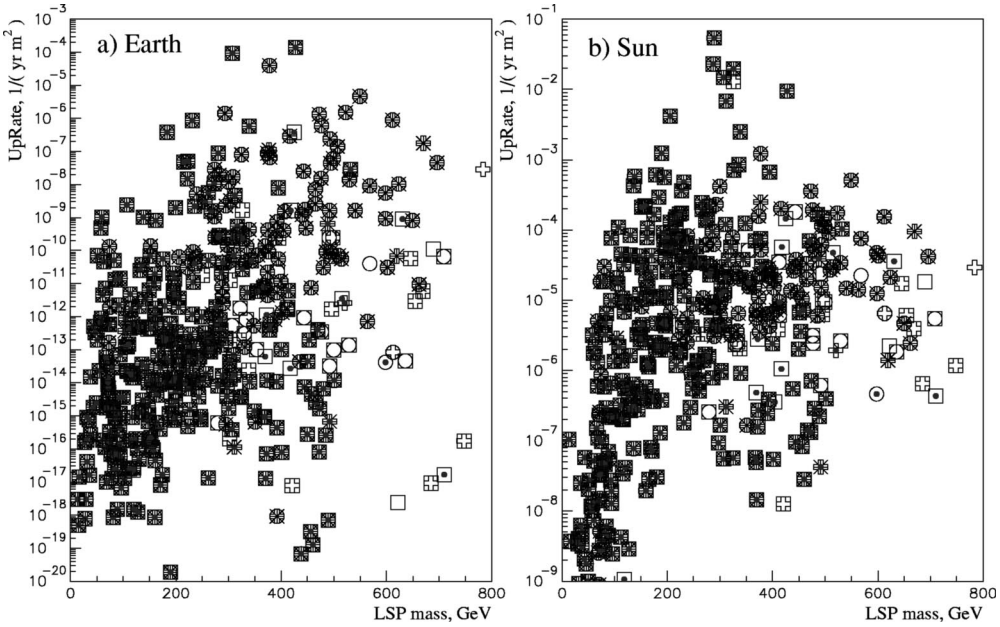

FIG. 7. Indirect detection rate for upgoing muons from $\chi\chi$ annihilation in the Earth (a) and the Sun (b). As in Fig. 5, stars, crosses, circles, small dots, and squares correspond to $0.1<\Omega h^2{}_{\rm IGC}, \Omega h^2{}_{\rm SQC}, \Omega h^2{}_{\rm SLC}, \Omega h^2{}_{\rm NCC}, \Omega h^2{}_{\rm ACC}<0.3$, respectively. NCC decreases the detection rates for models with $m_\chi \geqslant 400$ GeV.

B. Coannihilation effects in the detection rates

Now we consider the influence of all possible coannihilation channels (NCC, SQC, and SLC) on prospects for indirect and direct detection of CDM neutralinos. The results of our calculations (scatter plots) for cold dark matter observables are presented in Figs. 7–9. We compare the rate predictions for cosmologically interesting LSPs when the RD is evaluated with or without any of coannihilation channels taken into account. We see (Fig. 5) that in most models with $m_\chi \leqslant 250$ GeV the RD is unaffected by SQC, SLC, and NCC, mostly because the difference $m_{\rm NLSP}-m_\chi$ is too large to yield significant effects, therefore the corresponding detection rates are not influenced (depicted in the figures as a square filled with a star, a cross, and a dot simultaneously).

Figure 7 displays the expected indirect detection rates for upgoing muons produced in the Earth by neutrinos from decay products of $\chi\chi$ annihilation which takes place in the core of the Earth or of the Sun.

For $\chi\chi$ annihilation in the Earth upgoing muon detection rates merely lie within the range 10^{-19} m$^{-2}\cdot$yr$^{-1}<\Gamma^\mu<5$

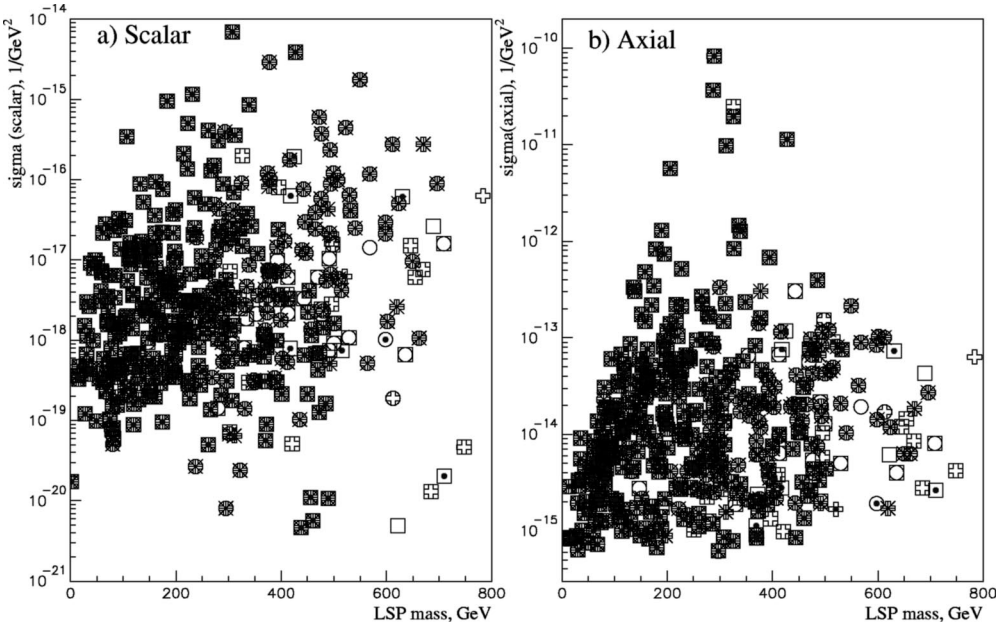

FIG. 8. Neutralino-proton scattering cross sections for scalar (spin-independent) interaction (a) and axial (spin-dependent) interaction (b). The notations are as in Fig. 7.

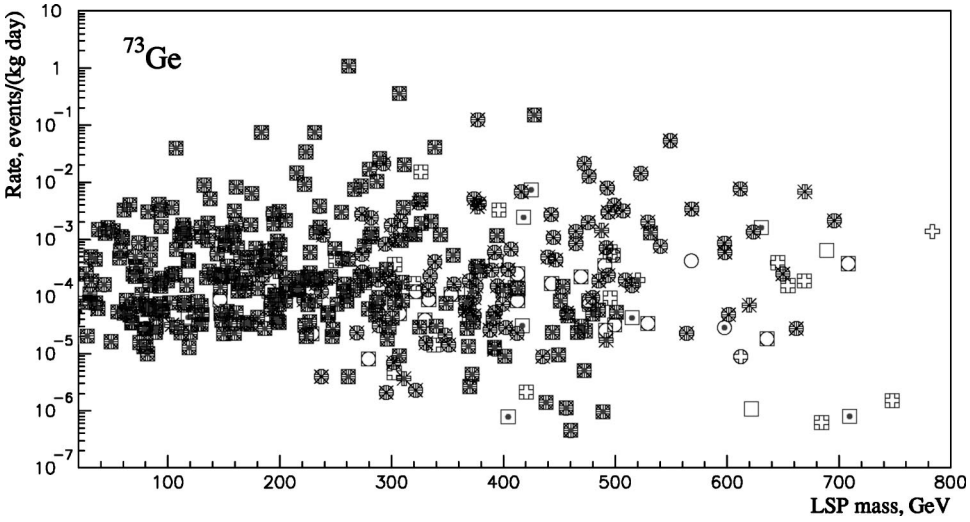

FIG. 9. Event rate for direct neutralino detection in a ^{73}Ge detector. As in Fig. 5, stars, crosses, circles, small dots, and squares correspond to $0.1<\Omega h^2_{\rm IGC}$, $\Omega h^2_{\rm SQC}$, $\Omega h^2_{\rm SLC}$, $\Omega h^2_{\rm NCC}$, $\Omega h^2_{\rm ACC}<0.3$, respectively. NCC decreases the maximal event rates for models with $m_\chi \geqslant 500$ GeV, but the models with smaller LSP mass are unaffected by the coannihilations.

$\times 10^{-5}$ m$^{-2}\cdot$yr^{-1} as long as $m_\chi \leqslant 250$ GeV. When $m_\chi \geqslant 250$ GeV, some of the models with $0.1<\Omega h^2_{\rm IGC}<0.3$ are removed from the cosmological interesting range ($\Omega h^2_{\rm COA}<0.1$; Fig. 5) mainly due to NCC (Fig. 7). Other models with $\Omega h^2_{\rm IGC}>0.3$ are shifted into this region (Fig. 5 and Fig. 7) mainly due to SLC and SQC. For $m_\chi \geqslant 250$ GeV one finds 10^{-19} m$^{-2}\cdot$yr$^{-1}<\Gamma^\mu_{\rm ACC}<5\times 10^{-7}$ m$^{-2}\cdot$yr^{-1} when the RD is evaluated with coannihilations taken into account, and 10^{-19} m$^{-2}\cdot$yr$^{-1}<\Gamma^\mu_{\rm IGC}<4\times 10^{-6}$ m$^{-2}\cdot$yr^{-1} when coannihilations are neglected. The large values of the detection rates of $\chi\chi$ annihilation in the Earth are decreased (from 10^{-5} m$^{-2}\cdot$yr^{-1} to 10^{-8} m$^{-2}\cdot$yr^{-1}) only for heavy LSPs, $m_\chi>450$ GeV, in accordance with the fact that the corresponding models are removed from the cosmologically interesting range. The SQC does not significantly change this conclusion obtained in [42] for SLC and NCC.

In the case of indirect detection of upgoing muons from $\chi\chi$ annihilation in the Sun one has generally similar behavior for models with $m_\chi \geqslant 350$ GeV. The only noticeable difference is in the absolute predictions for detection rates for models with $m_\chi>500$ GeV, where instead of $\Gamma^\mu_{\rm IGC}<10^{-4}$ m$^{-2}\cdot$yr^{-1} one expects the rates to be $\Gamma^\mu_{\rm ACC}<3\times 10^{-5}$ m$^{-2}\cdot$yr^{-1}. The highest predicted detection rates of 10^{-1}m$^{-2}\cdot$yr^{-1} are again correlated to a few models which are unaffected by coannihilation [42]. The SQC does not significantly contribute to reduction of the rates.

Figure 8 shows neutralino-proton scattering cross sections for the scalar (spin-independent) and axial (spin-dependent) interactions. As in the previous figures, the models with $m_\chi \leqslant 250$ GeV are hardly affected by coannihilation, and for the majority of those models both neutralino-proton and neutralino-neutron scattering cross sections reach values $\sigma_{\chi p}\leqslant 10^{-17}$ GeV^{-2} with the maximal cross section of the order of 10^{-15} GeV^{-2}.

Cosmologically interesting models with $m_\chi \geqslant 250$ GeV were influenced by coannihilations in the way discussed above, and the maximal value of the neutralino-nucleon cross section decreases from 10^{-15} GeV^{-2} to 10^{-16} GeV^{-2} for the models with $m_\chi>500$ GeV. All in all independently of neglecting or including of NCC, SQC, and SLC, the maximal scalar scattering neutralino-nucleon cross section was large as $10^{-15}-10^{-14}$ GeV^{-2}.

The spin-dependent neutralino-nucleon cross sections are typically higher than the spin-independent ones, and we have found the maximal values 10^{-10} GeV^{-2} for the axial neutralino-proton and 10^{-11} GeV^{-2} for the axial neutralino-neutron scattering for the models which are unaffected by the coannihilations. The majority of cosmologically interesting models yield axial neutralino-proton scattering cross sections in the range 5×10^{-16} GeV$^{-2}<\sigma_{\chi p}<2\times 10^{-12}$ GeV^{-2} and axial neutralino-neutron scattering cross sections in the range 2×10^{-16} GeV$^{-2}<\sigma_{\chi n}<8\times 10^{-13}$ GeV^{-2} [42]. The SQC contributes to the reduction of the cross sections, but not significantly again.

Due to the fact that capture of χ in the Sun (contrary to the Earth) occurs also via spin-dependent χp interaction, there are noticeable correlations between the highest upgoing muon rates from $\chi\chi$ annihilation in the Sun and the highest values of the axial neutralino-proton scattering cross sections [Figs. 7(b) and 8(b)].

Figure 9 shows the expected direct detection event rates calculated for a ^{73}Ge detector when NCC, SQC, SLC, and ACC are taken into account. For models with $m_\chi \leqslant 250$ GeV coannihilations of any kind play no role. The estimations of the event rate for models with $m_\chi \geqslant 400$ GeV are decreased [to about 0.005 event/(kg day)] due to NCC [42].

IV. CONCLUSION

Due to continuing improvements of the accuracy of astrophysical data and the importance of relic density constraints for SUSY models the precision calculation of the neutralino relic density is very desirable. The progress in this direction is very fast. Recently a new sophisticated C code MICROMEGAS on the basis of COMPHEP [52] for calculations of the relic density in the MSSM has been presented [27]. It includes all coannihilation channels with neutralinos, charginos, sleptons, squarks and gluinos. The relic density of neutralinos in the MSUGRA was calculated on the basis of annihilation diagrams involving sleptons, charginos, neutralinos, and third generation squarks in [37]. This paper is

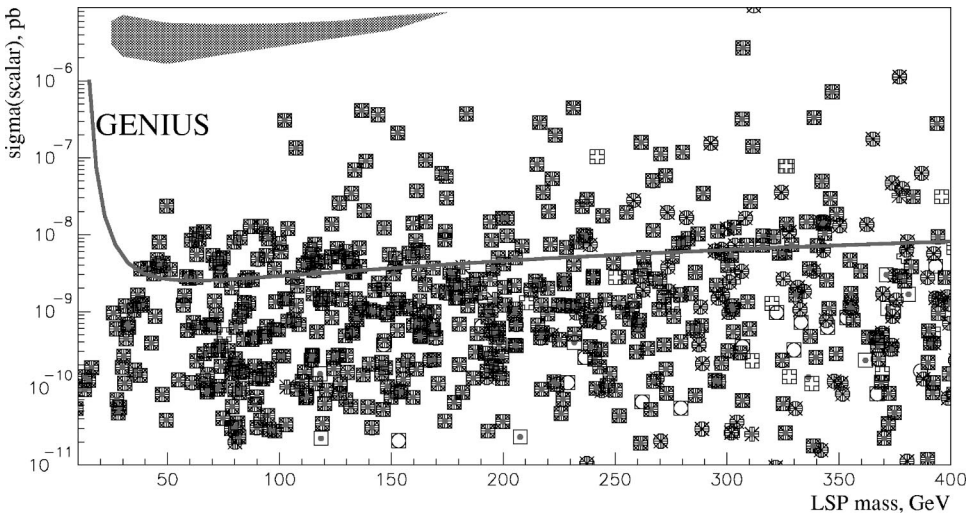

FIG. 10. Neutralino-proton scattering cross sections for scalar (spin-independent) interaction. The notations are as in Fig. 7. Expectations for the GENIUS detector [54] and the annual-modulation region of DAMA (shaded region) [55] are also given. The maximal sensitivity of GENIUS and the region of DAMA are located at $40 \leqslant m_\chi \leqslant 300$ GeV.

mostly devoted to prospects for SUSY search with various e^+e^- and hadron colliders and pays no attention to the individual contributions of different coannihilation channels. In addition, a full set of exact, analytic expressions for the annihilation of the lightest neutralino pairs [38] as well as slepton-neutralino coannihilations [40] into all two-body tree-level final states in the framework of minimal SUSY is now available. The authors of the DARKSUSY have also made new efforts [53] to include all possible channels of coannihilations in their publicly available DARKSUSY code.

Following this main direction we calculated the neutralino relic density (RD) taking into account slepton-neutralino (SLC), neutralino-chargino/neutralino (NCC), and squark-neutralino (SQC)coannihilation channels within the low-energy effective MSSM. To this end we have implemented in our code [43] the relic density part (with neutralino-chargino coannihilations) of the DARKSUSY code [24] supplied with the adopted code of [26] (calculating slepton-neutralino coannihilations) and the generalized (including sbottom-neutralino coannihilations) code of [34] (calculating top-squark–neutralino coannihilations). With the help of this new code, in contrast with previous considerations, we pay attention to the interplay between different coannihilation channels in the effMSSM.

We have shown that in the effMSSM the maximum factors of the RD decrease due to NCC as well as due to SQC and SLC can reach 10^{-3}, as long as the lower experimental limits for $m_{\tilde{\tau}}$, $m_{\tilde{l}}$, $m_{\tilde{b}}$, and $m_{\tilde{\chi}^\pm}$ are of the order of 80 GeV. We conclude that SQC, NCC, SLC produce comparable RD reduction effects in the effMSSM. For the majority of models which are affected by coannihilations and which successfully passed all relevant accelerator, cosmological, and rare-decay constraints it was observed that either NCC, SQC, or SLC alone produces a significant reduction of the RD while the other coannihilation channels give considerably smaller or zero further reduction. Contrary to NCC and SLC, which produce non-negligible effects only if the NLSP mass is smaller than $1.15m_\chi$, for SQC the relevant NLSP mass could reach $1.50m_\chi$. The type of NLSP determines the dominant coannihilation channel [42]. Due to the fact that the effMSSM more often favors neutralinos and charginos, but not sfermions, to be the NLSP (the NLSP-LSP mass differences in general are systematically larger for sfermions than for gauginos), the NCC channel more often dominantes in agreement with [23]. Only LSPs with the gaugino fraction $\mathcal{P} > 0.7$ remain CDM candidates of cosmological interest.

Some models for which $\Omega h^2 > 0.3$ when coannihilations is neglected fall within the cosmologically interesting region merely due to SLC and SQC, and some other models shift out of the region below $\Omega h^2 < 0.1$ merely due to NCC. In the effMSSM, contrary to MSUGRA [26], all coannihilations do not impose new cosmological limits on the mass of the LSP [42]. The optimistic predictions for neutralino-nucleon cross sections and indirect and direct detection rates for cosmologically interesting models are almost unaffected by these coannihilations. Only for large $m_\chi \geqslant 400$ GeV, the respectively high values are reduced, mainly because the NCC excludes the corresponding models from the cosmological interesting region $0.1 < \Omega h^2_{\mathrm{IGC}} < 0.3$.

Therefore, future increase of the lower mass limits for all possible NLSPs [at the Fermilab Tevatron or CERN Large Hadron Collider (LHC)] can, in principle, strongly reduce the importance of the effect of any of the coannihilation channels. Furthermore, we would like to note that despite the obvious importance of sophisticated RD calculations, including complete sets of coannihilation channels, it may happen that coannihilations play no role at least for the *direct* detection of cold dark matter. From Fig. 10 one can see that the field of maximal sensitivity of the best new-generation CDM detectors, such as GENIUS [54], as well as the annual-modulation region of DAMA [55] are located at $40 \leqslant m_\chi \leqslant 300$ GeV, where coannihilation effects are almost invisible.

ACKNOWLEDGMENTS

The authors thank Yudi Santoso for making his code available and I.V. Krivosheina for permanent interest in the work. V.B. thanks the Max Planck Institut fuer Kernphysik for the hospitality and the RFBR (Grants 00–02–17587 and 02–02–04009) for support.

[1] P. de Bernardis, Nature (London) **404**, 955 (2000); A. Balbi *et al.*, Astrophys. J. Lett. **545**, L1 (2000); **558**, L145(E) (2001).
[2] E.W. Kolb and M.S. Turner, *The Early Universe* (Addison-Wesley, Reading, MA, 1990); M.S. Turner, astro-ph/0108103.
[3] G. Jungman, M. Kamionkowski, and K. Griest, Phys. Rep. **267**, 195 (1996).
[4] H.P. Nilles, Phys. Rep. **110**, 1 (1984); H.E. Haber and G. Kane, *ibid.* **117**, 75 (1985); S. Martin, hep-ph/9709356.
[5] MAXIMA Collaboration, A.T. Lee *et al.*, Astrophys. J. Lett. **561**, L1 (2001); BOOMERANG Collaboration, C.B. Netterfield *et al.*, Astrophys. J. **571**, 604 (2002); DASI Collaboration, N.W. Halverson *et al.*, *ibid.* **568**, 38 (2002); P. de Bernardis *et al.*, *ibid.* **564**, 559 (2002); A. Melchiorri, astro-ph/0201237.
[6] H. Goldberg, Phys. Rev. Lett. **50**, 1419 (1983).
[7] J. Ellis, J. Hagelin, D. Nanopoulos, and M. Srednicki, Phys. Lett. **127B**, 233 (1983); J. Ellis, J. Hagelin, D. Nanopoulos, K. Olive, and M. Srednicki, Nucl. Phys. **B238**, 453 (1984).
[8] L.M. Krauss, Nucl. Phys. **B227**, 556 (1983).
[9] K. Griest, Phys. Rev. D **38**, 2357 (1988); **39**, 3802(E) (1989).
[10] K. Griest, M. Kamionkowski, and M. Turner, Phys. Rev. D **41**, 3565 (1990).
[11] J. Ellis, L. Roszkowski, and Z. Lalak, Phys. Lett. B **245**, 545 (1990).
[12] K.A. Olive and M. Srednicki, Phys. Lett. B **230**, 78 (1989); Nucl. Phys. **B355**, 208 (1991).
[13] M. Drees and M. Nojiri, Phys. Rev. D **47**, 376 (1993).
[14] K. Griest and D. Seckel, Phys. Rev. D **43**, 3191 (1991).
[15] P. Gondolo and G. Gelmini, Nucl. Phys. **B360**, 145 (1991).
[16] R. Arnowitt and P. Nath, Phys. Rev. Lett. **69**, 725 (1992); P. Nath and R. Arnowitt, *ibid.* **70**, 3696 (1993); Phys. Lett. B **437**, 344 (1998).
[17] J.L. Lopez, D.V. Nanopoulos, and K. Yuan, Phys. Rev. D **48**, 2766 (1993).
[18] M. Srednicki, R. Watkins, and K. Olive, Nucl. Phys. **B310**, 693 (1988).
[19] H. Baer and M. Brhlik, Phys. Rev. D **53**, 597 (1996); **57**, 567 (1998); H. Baer *et al.*, *ibid.* **63**, 015007 (2001).
[20] R. Barbieri, M. Frigeni, and G.F. Giudice, Nucl. Phys. **B313**, 725 (1989).
[21] A. Bottino, V. de Alfaro, N. Fornengo, G. Mignola, and S. Scopel, Astropart. Phys. **1**, 61 (1992); A. Bottino *et al.*, *ibid.* **2**, 67 (1994); V. Berezinsky *et al.*, *ibid.* **5**, 1 (1996); A. Bottino, F. Donato, N. Fornengo, and S. Scopel, Phys. Rev. D **59**, 095004 (1999).
[22] J. Ellis and L. Roszkowski, Phys. Lett. B **283**, 252 (1992); L. Roszkowski and R. Roberts, *ibid.* **309**, 329 (1993); G. Kane, C. Kolda, L. Roszkowski, and J. Wells, Phys. Rev. D **49**, 6173 (1994).
[23] J. Edsjo and P. Gondolo, Phys. Rev. D **56**, 1879 (1997); Phys. At. Nucl. **61**, 1181 (1998); P. Gondolo and J. Edsjo, hep-ph/9804459; J. Edsjo, hep-ph/9704384.
[24] P. Gondolo, J. Edsjö, L. Bergström, P. Ullio, and E.A. Baltz, astro-ph/0012234; http://www.physto.se/edsjo/darksusy/
[25] J.R. Ellis, T. Falk, G. Ganis, K.A. Olive, and M. Srednicki, Phys. Lett. B **510**, 236 (2001).
[26] J.R. Ellis, T. Falk, and K.A. Olive, Phys. Lett. B **444**, 367 (1998); J.R. Ellis, T. Falk, K.A. Olive, and M. Srednicki, Astropart. Phys. **13**, 181 (2000); **15**, 413 (2000).
[27] G. Belanger, F. Boudjema, A. Pukhov, and A. Semenov, Comput. Phys. Commun. **149**, 103 (2002).
[28] M.E. Gomez, G. Lazarides, and C. Pallis, Phys. Lett. B **487**, 313 (2000); Phys. Rev. D **61**, 123512 (2000).
[29] M.E. Gomez and J.D. Vergados, Phys. Lett. B **512**, 252 (2001).
[30] A.B. Lahanas, D.V. Nanopoulos, and V.C. Spanos, Phys. Rev. D **62**, 023515 (2000).
[31] R. Arnowitt, B. Dutta, and Y. Santoso, Nucl. Phys. **B606**, 59 (2001); R. Arnowitt and B. Dutta, hep-ph/0112157.
[32] A. Corsetti and P. Nath, Phys. Rev. D **64**, 125010 (2001); hep-ph/0005234.
[33] C. Boehm, A. Djouadi, and M. Drees, Phys. Rev. D **62**, 035012 (2000).
[34] J.R. Ellis, K.A. Olive, and Y. Santoso, hep-ph/0112113.
[35] G. Belanger, F. Boudjema, A. Cottrant, R.M. Godbole, and A. Semenov, Phys. Lett. B **519**, 93 (2001).
[36] T. Nihei, L. Roszkowski, and R. Ruiz de Austri, J. High Energy Phys. **05**, 063 (2001).
[37] H. Baer, C. Balazs, and A. Belyaev, J. High Energy Phys. **03**, 042 (2002).
[38] T. Nihei, L. Roszkowski, and R. Ruiz de Austri, J. High Energy Phys. **03**, 031 (2002).
[39] S. Mizuta and M. Yamaguchi, Phys. Lett. B **298**, 120 (1993).
[40] T. Nihei, L. Roszkowski, and R. Ruiz de Austri, J. High Energy Phys. **07**, 024 (2002).
[41] Y. Santoso, hep-ph/0205026.
[42] V.A. Bednyakov, H.V. Klapdor-Kleingrothaus, and E. Zaiti, Phys. Rev. D **66**, 015010 (2002).
[43] V.A. Bednyakov and H.V. Klapdor-Kleingrothaus, Phys. Rev. D **63**, 095005 (2001); **62**, 043524 (2000); V.A. Bednyakov, H.V. Klapdor-Kleingrothaus, and H. Tu, *ibid.* **64**, 075004 (2001).
[44] Y.G. Kim, T. Nihei, L. Roszkowski, and R. Ruiz de Austri, hep-ph/0208069.
[45] For current status of CMSSM see J.R. Ellis, K. Olive, and Y. Santoso, New J. Phys. **4**, 32 (2002).
[46] A. Chamseddine, R. Arnowitt, and P. Nath, Phys. Rev. Lett. **49**, 970 (1982); R. Barbieri, S. Ferrara, and C. Savoy, Phys. Lett. **119B**, 343 (1982); L.J. Hall, J. Lykken, and S. Weinberg, Phys. Rev. D **27**, 2359 (1983).
[47] K. Hagiwara *et al.*, Phys. Rev. D **66**, 010001 (2002); http://pdg.web.cern.ch/pdg
[48] CLEO Collaboration, M.S. Alam *et al.*, Phys. Rev. Lett. **74**, 2885 (1995); Belle Collaboration, K. Abe *et al.*, hep-ex/0107065.
[49] S. Bertolini, F. Borzumati, A. Masiero, and G. Ridolfi, Nucl. Phys. **B353**, 591 (1991); R. Barbieri and G. Giudice, Phys. Lett. B **309**, 86 (1993); A.J. Buras *et al.*, Nucl. Phys. **B424**, 374 (1994); A. Ali and C. Greub, Z. Phys. C **60**, 433 (1993).
[50] Toby Falk (private communication).
[51] Yudi Santoso (private communication).
[52] A. Pukhov *et al.*, hep-ph/9908288; http://theory.sinp.msu.ru/~pukhov/calchep.html
[53] E.A. Baltz and P. Gondolo, astro-ph/0207673.
[54] H.V. Klapdor-Kleingrothaus, Int. J. Mod. Phys. A **13**, 3953 (1998); H.V. Klapdor-Kleingrothaus and Y. Ramachers, Eur.

Phys. J. A **3**, 85 (1998); H.V. Klapdor-Kleingrothaus *et al.*, ''GENIUS: A Supersentive Germanium Detector System for Rare Events,'' Proposal, MPI-H-V26-1999, 1999, hep-ph/9910205; H.V. Klapdor-Kleingrothaus, *Springer Tracts in Modern Physics* (Springer, Berlin, 2002), Vol. 163, p. 69; Nucl. Phys. B (Proc. Suppl.) **110**, 364 (2002).

[55] DAMA Collaboration, R. Bernabei *et al.*, Phys. Lett. B **480**, 23 (2000); Eur. Phys. J. C **18**, 283 (2000).